

UC Davis

UC Davis Previously Published Works

Title

PhOBF1, a petunia ocs element binding factor, plays an important role in antiviral RNA silencing.

Permalink

<https://escholarship.org/uc/item/13v25284>

Journal

Journal of experimental botany, 68(5)

ISSN

0022-0957

Authors

Sun, Daoyang
Li, Shaohua
Niu, Lixin
et al.

Publication Date

2017-02-01

DOI

10.1093/jxb/erw490

Peer reviewed



RESEARCH PAPER

***PhOBF1*, a petunia ocs element binding factor, plays an important role in antiviral RNA silencing**

Daoyang Sun^{1,2}, Shaohua Li¹, Lixin Niu¹, Michael S. Reid², Yanlong Zhang^{1,*} and Cai-Zhong Jiang^{2,3,*}

¹ Department of Landscape Architecture and Arts, Northwest A&F University, Yangling, Shaanxi 712100, China

² Department of Plant Sciences, University of California Davis, Davis, CA 95616, USA

³ Crops Pathology and Genetic Research Unit, United States Department of Agriculture, Agricultural Research Service, Davis, CA 95616, USA

* Correspondence: zhangyanlong@nwsuaf.edu.cn and cjiang@ucdavis.edu

Received 7 October 2016; Editorial decision 9 December 2016; Accepted 9 December 2016

Editor: Lars Hennig, Swedish University of Agricultural Sciences

Abstract

Virus-induced gene silencing (VIGS) is a common reverse genetics strategy for characterizing the function of genes in plants. The detailed mechanism governing RNA silencing efficiency triggered by viruses is largely unclear. Here, we reveal that a petunia (*Petunia hybrida*) ocs element binding factor, *PhOBF1*, one of the basic leucine zipper (bZIP) transcription factors, was up-regulated by Tobacco rattle virus (TRV) infection. Simultaneous silencing of *PhOBF1* and a reporter gene, *phytoene desaturase* (*PDS*) or *chalcone synthase* (*CHS*), by TRV-based VIGS led to a failure of the development of leaf photobleaching or the white-corollas phenotype. *PhOBF1* silencing caused down-regulation of RNA silencing-related genes, including RNA-dependent RNA polymerases (*RDRs*), Dicer-like RNase III enzymes (*DCLs*), and Argonautes (*AGOs*). After inoculation with the TRV-*PhPDS*, *PhOBF1*-RNAi lines exhibited a substantially impaired *PDS* silencing efficiency, whereas overexpression of *PhOBF1* resulted in a recovery of the silencing phenotype (photobleaching) in systemic leaves. A compromised resistance to TRV and Tobacco mosaic virus was found in *PhOBF1*-RNAi lines, while *PhOBF1*-overexpressing lines displayed an enhanced resistance to their infections. Compared with wild-type plants, *PhOBF1*-silenced plants accumulated lower levels of free salicylic acid (SA), salicylic acid glucoside, and phenylalanine, contrarily to higher levels of those in plants overexpressing *PhOBF1*. Furthermore, transcripts of a number of genes associated with the shikimate and phenylpropanoid pathways were decreased or increased in *PhOBF1*-RNAi or *PhOBF1*-overexpressing lines, respectively. Taken together, the data suggest that *PhOBF1* regulates TRV-induced RNA silencing efficiency through modulation of *RDRs*, *DCLs*, and *AGOs* mediated by the SA biosynthesis pathway.

Key words: Phenylpropanoid pathways, salicylic acid biosynthesis, shikimate, tobacco mosaic virus, tobacco rattle virus, transcription factor, virus-induced gene silencing.

Introduction

Virus-induced gene silencing (VIGS), related to post-transcriptional gene silencing, is an attractively fast approach for degradation of homologous RNA molecules in plants

(Reid *et al.*, 2009; Jiang *et al.*, 2011). This RNA silencing machinery employs a number of core components, including RNA-dependent RNA polymerases (*RDRs*), Dicer-like

RNase III enzymes (DCLs), and Argonautes (AGOs), to implement small interfering RNA (siRNA)-mediated gene knockdown in a sequence-specific manner (Schwach *et al.*, 2005; Jaubert *et al.*, 2011). The Arabidopsis genome contains four DCLs, six RDRs, and ten AGOs (Donaire *et al.*, 2008; Zhang *et al.*, 2012), respectively contributing to the siRNA biogenesis, double-stranded RNA (dsRNA) formation, and incorporation into an RNA-induced silencing complex.

DCL1 uniquely accounts for the generation of 21-nucleotide (nt) microRNAs (miRNAs), which functions as a crucial coordinator of intricate biological processes (Bartel and Bartel, 2003). The dsRNA structures can be precisely recognized and cleaved by DCL2, DCL3, and DCL4 into 22-, 24-, and 21-nt siRNAs (Donaire *et al.*, 2008; Axtell, 2013). Depletion of DCL2, DCL3, and DCL4 enhances susceptibility to infection by RNA viruses, including *Tobacco rattle virus* (TRV) (Deleris *et al.*, 2006), *Cucumber mosaic virus* (CMV), and *Turnip crinkle virus* (TCV) (Bouché *et al.*, 2006) in Arabidopsis. It has been noted that DCL2 and DCL4 appear to impose a principle influence on virus-induced RNA silencing, whereas DCL3 acts as a minor regulator in antiviral silencing (Qu *et al.*, 2008; Garcia-Ruiz *et al.*, 2010). Plants use multiple RDR host pathways to generate viral secondary siRNAs by re-amplifying the cleaved single-stranded (ss) RNA complementary to the siRNA, which therefore favors the improvement of the silencing effect (Molnar *et al.*, 2010; Alvarado and Scholthof, 2011). Moreover, RDR1, RDR2, and RDR6 are implicated in defense against various RNA viruses via production of viral secondary siRNAs (Donaire *et al.*, 2008; Wang *et al.*, 2010). For instance, the mutants lacking RDR1, RDR2, and RDR6 exhibit a compromised resistance to *Turnip mosaic virus* (TuMV) infection in Arabidopsis (Garcia-Ruiz *et al.*, 2010). With respect to AGOs, AGO1 plays a major role in the miRNA silencing pathway (Baumberger and Baulcombe, 2005), which controls endogenous genes in terms of development, hormone regulation and stress response (Voinnet, 2009). Current evidence has uncovered the importance of AGO1 in the RNA silencing mechanism for transcriptional regulation as well as in antiviral responses (Alvarado and Scholthof, 2011). In contrast to AGO1, AGO2 seems to be a more essential factor in RNA silencing and combat for viruses. AGO2 mutation leads to an impaired resistance to invasion by CMV (Wang *et al.*, 2011), TCV (Harvey *et al.*, 2011), *Potato virus X* (PVX) (Jaubert *et al.*, 2011), and *Tomato bushy stunt virus* (Scholthof *et al.*, 2011) in Arabidopsis or *Nicotiana benthamiana*. To date, however, how these RNA silencing components are transcriptionally regulated remains largely unknown.

Salicylic acid (SA) is an endogenous phytohormone required for induction of systemic acquired resistance (Malamy *et al.*, 1990). Inoculation with viral and non-viral pathogens results in increased SA accumulation (Kumar and Klessig, 2003). Exogenous application of SA inhibits virus proliferation of CMV, *Tobacco mosaic virus* (TMV), and TCV in Arabidopsis, tomato, tobacco and hot pepper (Shang *et al.*, 2011). Previous studies revealed two separated pathways, the isochorismate and phenylalanine ammonia lyase pathways, for SA biosynthesis in Arabidopsis (D'Maris

Amick Dempsey *et al.*, 2011). Both pathways initiate from chorismate, which is the ultimate product of the shikimate pathway. The aromatic amino acid phenylalanine is synthesized also through the shikimate pathway (Tzin and Galili, 2010). Some of the synthesized SAs are converted into conjugated SA glucosides (SAGs) functioning as an inactive form, from which free SA can be released (Rivas-San Vicente and Plasencia, 2011). To date, the research concerning SA has mainly focused on plant defense signaling against abiotic and biotic elicitors. Several lines of evidence support that a close correlation between SA-mediated viral defense and RNA silencing pathways may exist in plants. Exposure to SA markedly promotes the activity of NtRdRP in tobacco plants (Xie *et al.*, 2001). Silencing suppressor of CMV disrupts both RNA silencing and SA-mediated resistance to virus infection (Ji and Ding, 2001). SA-deficient transgenic tobacco plants exhibit a reduced accumulation of *Plum pox virus*-derived small RNAs, demonstrating that SA may serve as an enhancer of antiviral RNA silencing (Alamillo *et al.*, 2006). The latest findings indicate that transcripts of *RDR1*, *RDR2*, *DCL1*, and *DCL2* are up-regulated in tomato plants following *Citrus exocortis viroid* (CEVd), *Tomato mosaic virus* (ToMV) infection, and SA treatment (Campos *et al.*, 2014).

The basic leucine zipper (bZIP) proteins constitute a large transcription factor family in eukaryotes (Riechmann *et al.*, 2000). In Arabidopsis, the bZIP family is classified into ten subfamilies (A–I, S), of which the subfamily S is the largest group including 17 members (Jakoby *et al.*, 2002). AtbZIP11 belongs to subfamily S and its translation is suppressed by sucrose targeting a conserved upstream open reading frame region in the 5' untranslated regions of mRNA (Wiese *et al.*, 2004). AtbZIP11 regulates amino acid metabolism by directly interacting with *asparagine synthetase 1* (*ASN1*) and *proline dehydrogenase 2* (*ProDH2*) (Hanson *et al.*, 2008). Activation of AtbZIP11 leads to reprogramming of amino acid and sugar metabolism, leading to increased levels of phenylalanine, tryptophan, tyrosine, sucrose, fructose, and glucose, and reduced levels of trehalose, as well as promoting expression of corresponding metabolism-associated genes (Ma *et al.*, 2011). Plant growth is inhibited in Arabidopsis plants constitutively expressing AtbZIP11 via the regulatory mechanism associating with the sucrose non-fermenting-1-related protein kinase 1 and trehalose 6-phosphate signaling systems (Ma *et al.*, 2011). In addition, AtbZIP11 specifically activates the transcription of auxin-responsive genes via recruitment of histone acetylation machinery and contributes to the modulation of auxin-mediated responses (Weiste and Dröge-Laser, 2014). Moreover, *tbz17* in tobacco, *lip19* and *OsOBF1* in rice, and *mlip15* in maize are phylogenetically close to AtbZIP11. Transcript levels of *tbz17* (Kusano *et al.*, 1998), *lip19* (Shimizu *et al.*, 2005), and *mlip15* (Kusano *et al.*, 1995) are significantly increased under low temperature stress, while *OsOBF1* shows an opposite expression pattern (Shimizu *et al.*, 2005). In *N. babacum*, transcripts of *tbz17* are up-regulated during leaf senescence (Yang *et al.*, 2001). Overexpression of *tbz17* results in enlarged leaf cells and increased sucrose levels compared with wild-type (WT) (Thalor *et al.*, 2012). But the roles of bZIP11 in antiviral RNA silencing still remain enigmatic.

In previous studies, we obtained numerous up-regulated genes, including a large number of transcription factors, during flower development through transcriptomic analysis related to flower senescence in petunia (Wang *et al.*, 2013). We have successfully used a TRV-based VIGS method to assess the function of senescence-related genes in petunia floral tissues (Chen *et al.*, 2004; Reid *et al.*, 2009; Jiang *et al.*, 2011; Chang *et al.*, 2014; Yin *et al.*, 2015). However, when the TRV-*PhCHS* report system was employed to silence several candidate genes, the inoculated plants failed to show the expected white-petal phenotype of *CHS* silencing in the purple-petal petunia plants. Of the candidate genes, we have recently reported an ethylene-responsive element binding factor, *PhERF2*, which plays a critical role in TRV-induced RNA silencing and antiviral defense via transcriptional modulation of *RDR2*, *RDR6*, *DCL2*, and *AGO2* in petunia (Sun *et al.*, 2016). In this study, we report another regulatory gene, an ocs element binding factor of bZIP transcription factors, namely *PhOBF1*. Simultaneous silencing of *PhOBF1* and reporter genes, *PDS* or *CHS*, led to a severe impairment of leaf photobleaching or white-flower phenotype in petunia. *PhOBF1* appears to play a crucial role in the antiviral RNA silencing process through the regulation of the SA biosynthesis pathway.

Materials and methods

Plant materials and growth conditions

Petunia (*Petunia × hybrida*) plants were maintained in a growth chamber at 25/20 °C day/night temperatures with a 16/8 h light/dark cycle. Four-leaf-stage plantlets of cultivar 'Primetime Blue' were inoculated with TRV constructs to silence *PhOBF1* in leaves and floral tissues. Stable transformation was obtained from 'Mitchell Diploid'. Four-week-old transgenic plant leaves were sampled to determine the transcript levels of *PhOBF1*, RNA silencing-related genes and genes in the SA biosynthesis pathway, as well as concentrations of SA, SAG, and phenylalanine. To further examine the impact of *PhOBF1* on silencing efficiency of the VIGS system, transgenic plants at the four-leaf stage were infiltrated with TRV-*PhPDS*. For multiple resistance analysis, 4-week-old WT and transformed seedlings were inoculated with TRV and TMV. For all studies of gene expression in virus assay, inoculated or uppermost unfolded leaves (the third or fourth leaf from terminal) were harvested and used for total RNA isolation. Tissue-specific expression analysis of *PhOBF1* was conducted using younger leaves, stems, and roots, and flowers at anthesis (separated into sepals, petals, pistils, and stamens) of 10-week-old 'Mitchell Diploid' plants. Corollas at day 1, 3, 5, and 7 post-anthesis were used to study *PhOBF1* expression profiles during flower senescence.

Identification of *PhOBF1*

The *PhOBF1* cDNA fragments were isolated by RT-PCR as previously described (Chang *et al.*, 2014). Corresponding amino acids were deduced by the translate tool of ExPASy (<http://web.expasy.org/translate/>). Its conserved domain was identified using an NCBI web server (<http://www.ncbi.nlm.nih.gov/Structure/cdd/wrpsb.cgi>). Homologous proteins from petunia and other species were found through NCBI BLAST (<http://blast.ncbi.nlm.nih.gov/>). Multiple sequence alignment was conducted by CLUSTALW (<http://www.genome.jp/tools/clustalw/>). A phylogenetic tree was constructed by means of MEGA4 (version 4.0.2) software.

Abiotic stress and hormone treatments

For the cold treatment, 3-week-old seedlings of 'Primetime blue' were placed in small vials with distilled water and maintained at

room temperature (control) and in a 4 °C room. For the salinity and dehydration treatments, the seedlings were inserted in vials containing 100 mM NaCl and no water, respectively. For the ethylene treatment, the seedlings were treated with 10 $\mu\text{l l}^{-1}$ of ethylene gas continuously in a sealed chamber. For other hormone treatments, the plants were placed in vials containing 50 μM ABA, 50 μM gibberellic acid (GA_3), 200 μM SA, or 200 μM methyl jasmonate (MeJA). Samples were collected at 0, 3, 6, 12, and 24 h post-treatment.

Construction of VIGS plasmids

The TRV-*PhPDS*, TRV-*PhCHS*, and TRV-*PhPDS/CHS* plasmids were generated previously using 138-bp *PDS* and 194-bp *CHS* fragments (Chen *et al.*, 2004). To generate the TRV-*PhPDS/OBF1*, TRV-*PhCHS/OBF1*, and TRV-*PhPDS/CHS/OBF1* constructs, the fragment of *PhOBF1* were PCR-amplified using specific primers F1R1 (Supplementary Table S1 at JXB online) and then cloned into three respective plasmids as mentioned above. A different fragment (fragment 2) of *PhOBF1* amplified by specific primers F2R2 (Supplementary Table S1) was cloned into TRV-*PhPDS/CHS*. Similarly, a *PhbZIP44* fragment was PCR-amplified to form TRV-*PhPDS/bZIP44*, TRV-*PhCHS/bZIP44*, and TRV-*PhPDS/CHS/bZIP44* constructs. Additionally, the TRV-green fluorescent protein (GFP) construct was kindly provided by Junping Gao from China Agricultural University (Beijing, China) (Tian *et al.*, 2014).

Agro-inoculation of TRV vectors

Agrobacterium tumefaciens strain GV3101 was electrotransformed with TRV1 and TRV2 plasmids. The transformed bacteria were cultured in LB media with 40 mg l^{-1} kanamycin, 20 mg l^{-1} gentamicin, 10 mM MES, and 20 μM acetosyringone for 48 h at 28 °C. The cells were harvested via centrifugation and then resuspended in inoculation buffer containing 10 mM MgCl_2 , 10 mM MES, and 200 μM acetosyringone to an OD_{600} of 4.0, followed by incubation at room temperature for 3–5 h. Subsequently, the *Agrobacterium* cultures containing TRV1 and TRV2 plasmids were mixed together in a 1:1 ratio. The bacterial mixture was applied to the abaxial side of petunia leaves using a 1-ml disposal needle-free syringe (Reid *et al.*, 2009; Jiang *et al.*, 2011). The *Agrobacterium* without transformation was used as mock control.

Semi-quantitative RT-PCR and quantitative real-time PCR

TRIzol reagent (Invitrogen, Carlsbad, CA, USA) was used to isolate total RNA from petunia leaves or flowers. Purification of RNA was performed using RNase-free DNase I (Promega, Madison, WI, USA). First-strand cDNA was synthesized from total RNA (2–5 μg) with SuperScript III reverse transcriptase (Invitrogen, Carlsbad, CA, USA). PCR was carried out using Taq DNA polymerase (Invitrogen, Carlsbad, CA, USA) according to the manufacturer's recommendations, and resulting PCR products were analysed by electrophoresis. *26S ribosomal RNA* served as an internal control (Chen *et al.*, 2004; Reid *et al.*, 2009). Quantitative real-time PCR was performed using the SYBR Green PCR Master Mix (2X) (Applied Biosystems, Foster City, CA, USA) as previously described (Liang *et al.*, 2014). A minimum of three biological replicates were used for determining transcript abundances of genes. Statistical significance of difference was evaluated by Duncan's multiple range test at a *P* value <0.05.

Northern blot assay

Total RNA was extracted from the systemic petunia leaves infected with TRV vectors and mock control using TRIzol reagent (Invitrogen, Carlsbad, CA, USA). Small RNAs with low molecular mass were further isolated with a solution containing polyethylene glycol (PEG8000) and NaCl as previously described (Wang *et al.*, 2004).

The ethidium bromide stained 5S rRNA was served as a loading control. Blot hybridization was conducted as previously described (Donaire *et al.*, 2008). For analysis of siRNAs derived from TRV-*PhPDS*, oligonucleotide probes corresponding to *PDS* insert (138 bp) in TRV2 vector were radiolabeled with [γ - 32 P]ATP using T4 polynucleotide kinase (Promega). Finally, relative siRNA accumulation was visualized through RNA blots exposed to autoradiographic film.

Generation of transgenic petunia plants

The full-length of the *PhOBF1* ORF sequence was PCR-amplified using the following primers: 5'-ATCTCGAGATGG CATCTTCTAGTGGA-3' (forward) with an *XhoI* restriction site and 5'-ATGAGCTCTCAATACTGATAGAACATAT-3' (reverse) with a *SacI* restriction site. The fragment was cloned into pGSA1403 vector to form the overexpression construct (Chang *et al.*, 2014; Yin *et al.*, 2015). For RNAi construct, the fragment (Supplementary Fig. S1A) of *PhOBF1* cDNA was amplified using the primers FIR1 (Supplementary Table S1) with addition of a sequence harboring *SpeI*-*AscI* and *BamHI*-*SwaI* restriction sites in the 5' end of forward and reverse primers, respectively. The resulting products were ligated into pGSA1285 vector in sense and antisense orientations. The plasmids for overexpression and RNAi constructs were transformed into *A. tumefaciens* strain LBA4404 by electroporation. Petunia cultivar 'Mitchell Diploid' was used for generation of transgenic plants using the leaf-disk transformation method (Wang *et al.*, 2013; Liang *et al.*, 2014). Positive transgenic plants were screened on MS plates supplemented with 100 mg l⁻¹ kanamycin (Estrada-Melo *et al.*, 2015; Yin *et al.*, 2015).

Measurement of SA, SAG, and phenylalanine

Petunia leaves (0.2–0.5 g) were ground to fine powder in liquid nitrogen using a mortar and pestle. Determination of free SA and SAG levels was performed using a method previously described (Lee *et al.*, 2011) with some minor changes. Methanol-formic acid (1 ml; 95:5) was used to extract the leaf tissues. Samples were vortexed and sonicated for 20 min for a complete homogenization. The mixture was centrifuged at 15 000 g for 10 min at 4 °C. The supernatant was filtered through a 0.45 μ m filter and then freeze-dried in a vacuum. The pellet was resuspended in 1 ml of 5% trichloroacetic acid. Free SA was extracted organically by supplementing 1 ml of ethylacetate-cyclopentane-isopropanol (50:50:1). The upper phase containing free SA was collected and analysed by the high-performance liquid chromatography (HPLC). The SAG-containing aqueous phase after free SA extraction was exposed to acidification treatment by hydrochloric acid to pH 1.0. Subsequent boiling of acidified solution for 30 min was implemented for the release of SA from conjugated forms. The released SA was measured as described above. For quantification of phenylalanine, the ground powder of leaves was extracted with 1 ml 60% methanol (v/v), 0.1% phosphoric acid (v/v) with 2% 3-methylsalicylic acid (w/v). Following sonication, centrifugation, and filtration, the clear solution was injected into a C₁₈ column for HPLC separation as reported previously (Janzik *et al.*, 2005). The HPLC assay was performed using an Agilent chromatograph (model 1100, Agilent Technologies, Santa Clara, CA, USA), equipped with a fluorescence detector. The pure SA and phenylalanine (Sigma-Aldrich, St Louis, MO, USA) were dissolved and used as reference standards.

Inoculation with TMV

Infectious sap in 0.1 M phosphate buffer (pH 7.0, 1:4 w/v) was prepared from TMV-infected leaves of *N. benthamiana*. Prior to inoculation, the fully expanded leaves of 4-week-old healthy petunia plantlets were dusted with 400 mesh carborundum powder. The TMV sap was used to inoculate the leaves by a mechanical method (Hull, 2009). Relative virus accumulation was checked by

quantitative real-time PCR analysis of transcript levels of TMV-CP, encoding coat protein of TMV.

Results

TRV infection, abiotic stresses and hormone treatments induce PhOBF1 expression

A 1029-bp cDNA corresponding to a putative ocs element binding factor 1 (*OBF1*) gene was isolated from a library constructed from petunia flower (Wang *et al.*, 2013). The deduced protein, annotated as PhOBF1, was phylogenetically closed to tomato (*Solanum lycopersicum*) SIOBF1, potato (*S. tuberosum*) StOBF1, and Arabidopsis AtbZIP11. These proteins share a conserved basic leucine zipper domain with a length of 63 amino acids (Supplementary Fig. S1). *PhOBF1* was constitutively expressed in leaves and roots at a higher level than in stem and floral tissues (Supplementary Fig. S2). To study the impact of TRV infection on *PhOBF1* expression, the *Agrobacterium* bearing TRV empty vector was used to inoculate the leaves of four-leaf-stage WT petunia seedlings. Transcript abundances of *PhOBF1* increased remarkably at 36 h post-inoculation (hpi) in inoculated leaves and 15 d post-inoculation (dpi) in systemically infected upper leaves, respectively (Fig. 1A, B). By contrast, the inoculation with non-transformed *Agrobacterium* (mock control) did not alter *PhOBF1* expression levels (Fig. 1A, B). Furthermore, transcript levels of *PhOBF1* increased following exposure to low temperature and drought stresses (Fig. 1C) and was also up-regulated following ABA, ethylene, GA₃, and SA treatments (Fig. 1D).

Simultaneous silencing of PhOBF1 and reporter genes disrupts VIGS efficiency

To investigate the function of *PhOBF1*, TRV-based VIGS with visual reporters of *PDS* and *CHS* was employed to knockdown *PhOBF1* expression in the leaves and flowers of petunia, respectively. The plants inoculated with mock and empty vector displayed the normal WT phenotype with green leaves (Fig. 2A) and purple corollas (Fig. 2B). TRV-*PhPDS*-infected systemic leaves showed a typical *PDS*-silenced photobleaching phenotype. However, TRV-*PhPDS/OBF1*-infected systemic leaves failed to show a photobleaching phenotype at 3 and 5 weeks post-inoculation (wpi) (Fig. 2A). To examine whether the failed photobleaching phenotype is only associated with the *PhOBF1* gene, a cDNA fragment from a paralog of *PhOBF1*, *PhbZIP44* (Supplementary Fig. S1B) was used for comparison. The plants infected with TRV-*PhPDS/bZIP44* showed a *PDS*-silenced photobleaching phenotype (Fig. 2A). To further confirm this finding, another visual reporter gene, *CHS*, was introduced. The *CHS*-silenced white-corollas phenotype, as shown in TRV-*PhCHS* and TRV-*PhCHS/bZIP44*, was not observed in the flowers infected by TRV-*PhCHS/OBF1* at 7 wpi (Fig. 2B). Furthermore, the 3' end fragment (Supplementary Fig. S1A) of *PhOBF1* cDNA was inserted into a tandem construct TRV-*PhPDS/CHS* for VIGS assay. Both systemic leaves and

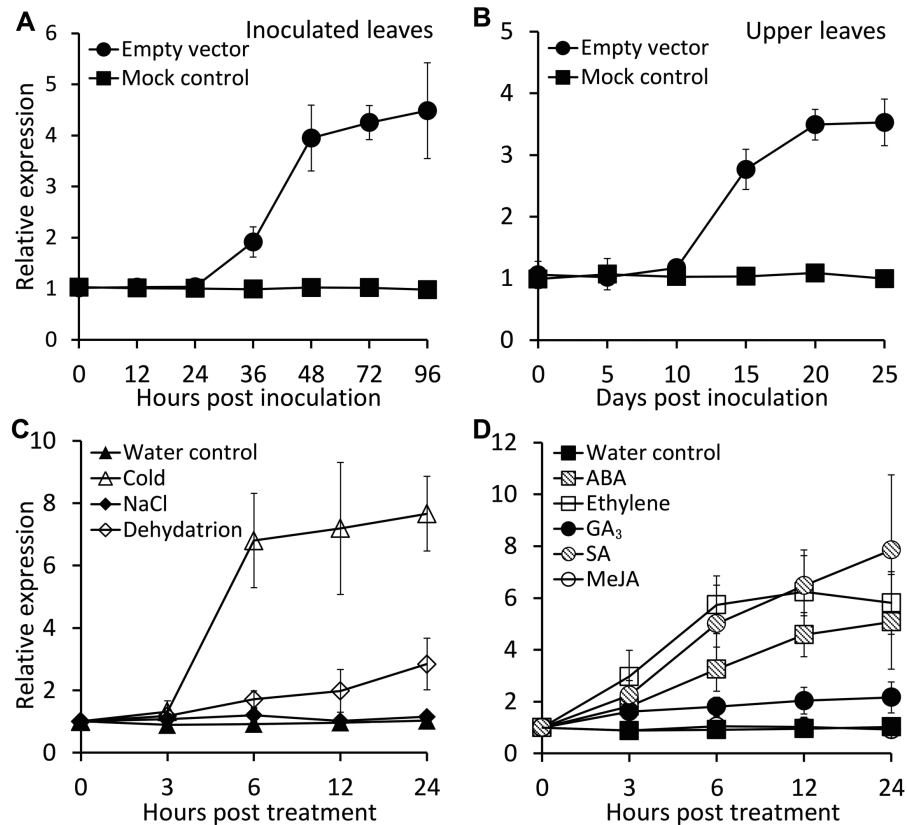


Fig. 1. Induction of *PhOBF1* expression by TRV infection, abiotic stresses and hormone treatments in petunia leaves. (A, B) Quantitative real-time PCR analysis of *PhOBF1* transcript levels in inoculated (A) and systemically infected upper (B) leaves with TRV at different time points. Four-week-old WT plants were inoculated with *Agrobacterium* bearing no TRV vector (mock control) or a TRV empty vector. (C, D) Quantitative real-time PCR analysis of *PhOBF1* transcript levels in response to abiotic stresses (C) and hormones (D) at different time points. Three-week-old petunia seedlings were placed in vials with water at room temperature (control) or in a 4 °C room (cold), or without water at room temperature (dehydration), or with 100 mM NaCl, 50 μ M ABA, 50 μ M GA₃, 200 μ M SA, or 200 μ M MeJA, or exposed to 10 μ l⁻¹ ethylene treatment. Transcript abundances were standardized to 26S *rRNA*. Error bars represent standard error of the mean from three biological replicates.

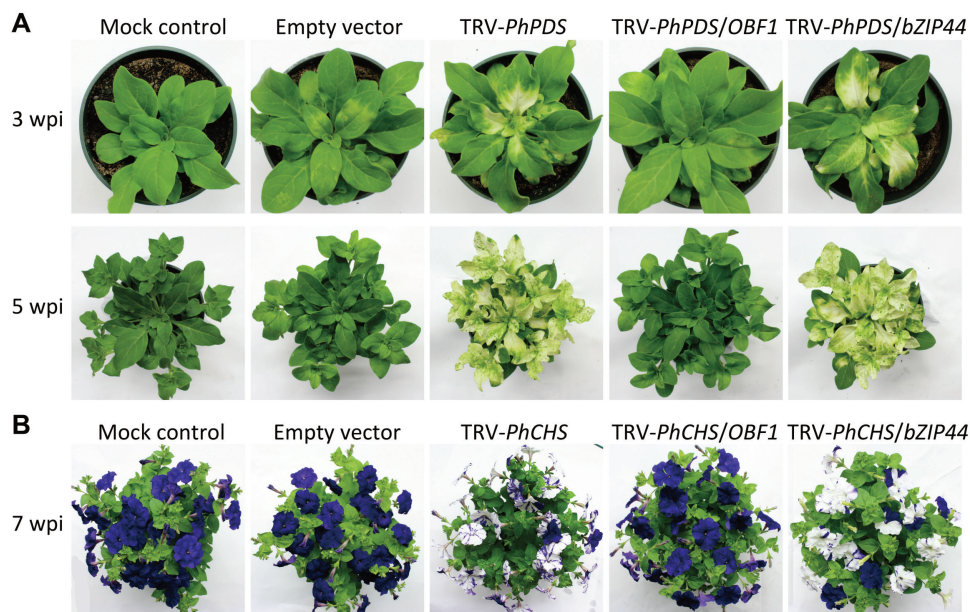


Fig. 2. Failed development of *PDS*-silenced leaf photobleaching and *CHS*-silenced white-corollas phenotypes in plants with *PhOBF1*-VIGS silencing. Representative phenotypes of WT plants at 3, 5 (A), and 7 (B) weeks post-inoculation (wpi) with *Agrobacterium* bearing no TRV vector (mock control), or a TRV empty vector, TRV-*PhPDS* and TRV-*PhCHS*, TRV-*PhPDS/OBF1* and TRV-*PhCHS/OBF1*, TRV-*PhPDS/bZIP44* and TRV-*PhCHS/bZIP44* constructs, respectively.

flowers from TRV-*PhPDS/CHS/OBF1* (F2)-infected plants did not show *PDS*-photobleaching and *CHS*-white silencing phenotypes during the entire growth periods (Supplementary Fig. S3).

VIGS silencing of PhOBF1 does not suppress virus proliferation

To understand why the inclusion of the *PhOBF1* fragment in TRV-*PhPDS* and TRV-*PhCHS* constructs severely impaired the *PDS*-silenced leaf photobleaching and *CHS*-silenced white-corollas phenotypes, we analysed transcript abundances of *PhOBF1* and *PDS*, and accumulation levels of TRV RNA1 and RNA2 in uppermost leaves of plants at 3 wpi. *PhOBF1* transcripts were up-regulated in the leaves from plants infected with TRV constructs except TRV-*PhPDS/OBF1* (Fig. 3A). The *PhOBF1* expression levels in leaves infected with TRV-*PhPDS/OBF1* were significantly lower than that in mock-treated leaves and other TRV construct-infected leaves (Fig. 3A), suggesting the partial knockdown of *PhOBF1* expression. When examining *PDS* transcripts, a significantly marked reduction (greater than 90%) was found in photobleached leaves from plants infected with TRV-*PhPDS* and TRV-*PhPDS/bZIP44* (Fig. 3A). However, only about a 40% reduction in *PDS* abundance was observed in leaves from TRV-*PhPDS/OBF1*-infected plants, compared with mock and empty vector controls (Fig. 3A).

Semi-quantitative RT-PCR analysis revealed that when two primer pairs covering multiple cloning sites (MCS) (RNA2-1) and a region upstream of MCS (RNA2-2) were used (Supplementary Table S1), DNA fragments carrying *PhOBF1* and *PDS* inserts were detected in TRV-*PhPDS/OBF1*-infected leaves (Fig. 3B), suggesting that the *PhOBF1* silencing did not suppress the TRV replication or movement. Quantitative real-time analysis indicated that the accumulation of TRV RNA1 in empty vector- and TRV-*PhPDS/OBF1*-infected leaves was significantly higher than that in the leaves of plants agro-infiltrated with TRV-*PhPDS* and TRV-*PhPDS/bZIP44* constructs (Fig. 3B).

VIGS silencing of PhOBF1 inhibits expression of RNA silencing-related genes and accumulation of siRNAs

To further understand failed detection of *PDS* and *CHS* silencing phenotypes in TRV-*PhPDS/OBF1*- and TRV-*PhCHS/OBF1*-infected plants, we examined transcript abundances of genes associated with the RNA silencing pathway. RDRs, DCLs and AGOs are indispensable components participating in dsRNA generation, cleavage and siRNA binding in the RNA silencing pathway (Burch-Smith *et al.*, 2006; Gould and Kramer, 2007; Jaubert *et al.*, 2011; Tian *et al.*, 2014). We measured the transcript abundances of *RDRs* (1, 2, 6), *DCLs* (1–4) and *AGOs* (1, 2) in uppermost leaves of plants at 3 wpi. The majority of the selected genes, except *RDR6*, *DCL3*, and *AGO1*, were significantly up-regulated in the leaves from empty vector-, TRV-*PhPDS*- or TRV-*PhPDS/bZIP44*-infected plants but not in TRV-*PhPDS/OBF1*-infected plants (Fig. 3C).

To determine TRV-*PhPDS*-derived siRNA abundance, northern blot analysis was performed using a DNA fragment of the *PDS* reporter as probe. No signals were detectable in the leaves from TRV-*PhPDS/OBF1*-infected plants. By comparison, one exclusive band with a length of 22 nt was detected in the leaves from plants infected with TRV-*PhPDS* and TRV-*PhPDS/bZIP44* (Fig. 3D).

PhOBF1 silencing by RNAi impairs VIGS efficiency

To better dissect *PhOBF1*'s function, transgenic petunia plants with down-regulated *PhOBF1* expression by RNAi were generated (lines 2, 6 and 8) and infected with TRV constructs. A striking impairment of the photobleaching phenotype was detected in the leaves of the transgenic plants infected with TRV-*PhPDS* reporter constructs (Fig. 4A), confirming the failed photobleaching phenotype in the VIGS assay. Transcript levels of *PhOBF1* in *PhOBF1*-RNAi lines were reduced by 70–80%, compared with WT (Fig. 4B). Accumulation levels of TRV RNA1 and RNA2 were higher in *PhOBF1*-silenced lines than that in WT plants infected with TRV-*PhPDS* (Fig. 4C). Following infection with TRV-*PhPDS*, approximately 90% reduction in *PDS* transcripts was found in WT leaves, whereas only 20–30% reduction in *PDS* transcripts was detected in *PhOBF1*-RNAi lines (Fig. 4C). Silencing of *PhOBF1* led to significant down-regulation of *RDR1*, *RDR2*, *DCL1*, *DCL2*, and *AGO2* in *PhOBF1*-RNAi, compared with the control lines (Fig. 4D). Transcript levels of *RDR6*, *DCL4*, and *AGO1* were slightly reduced in certain *PhOBF1*-RNAi lines (Fig. 4D). *PhOBF1* silencing did not affect transcript abundances of *DCL3* (Fig. 4D).

PhOBF1 overexpression restores silencing phenotype

To further study the function of *PhOBF1* in the RNA silencing process, we generated *PhOBF1*-overexpressing (OE) lines (B, D and H) in petunia. A prominent *PDS*-silenced leaf photobleaching phenotype emerged at 4 and 7 wpi in systemic leaves of WT and OE lines infected with TRV-*PhPDS* (Fig. 5A). A two- to three-fold increase in *PhOBF1* transcript levels was detected in three independent lines, compared with WT (Fig. 5B). TRV RNA1 and RNA2 accumulation was significantly decreased in *PhOBF1*-OE lines compared with WT (Fig. 5C). A dramatic and significant decrease in *PDS* transcript levels was found in the uppermost photobleached leaves of control and *PhOBF1*-OE lines infected with TRV-*PhPDS* at 4 wpi (Fig. 5C). Moreover, overexpression of *PhOBF1* significantly increased the transcript levels of *RDR1*, *RDR2*, *DCL1*, *DCL2*, *DCL4*, and *AGO2* in all transgenic lines (Fig. 5D). Overexpression of *PhOBF1* did not affect transcript abundances of *RDR6*, *DCL3*, and *AGO1*.

PhOBF1 affects plant defense against TRV and TMV

To examine the role of *PhOBF1* in plant defense against viral infections, a TRV vector expressing green fluorescent protein (TRV-GFP) (Tian *et al.*, 2014) was used to inoculate transgenic and WT leaves to visualize the accumulation of TRV

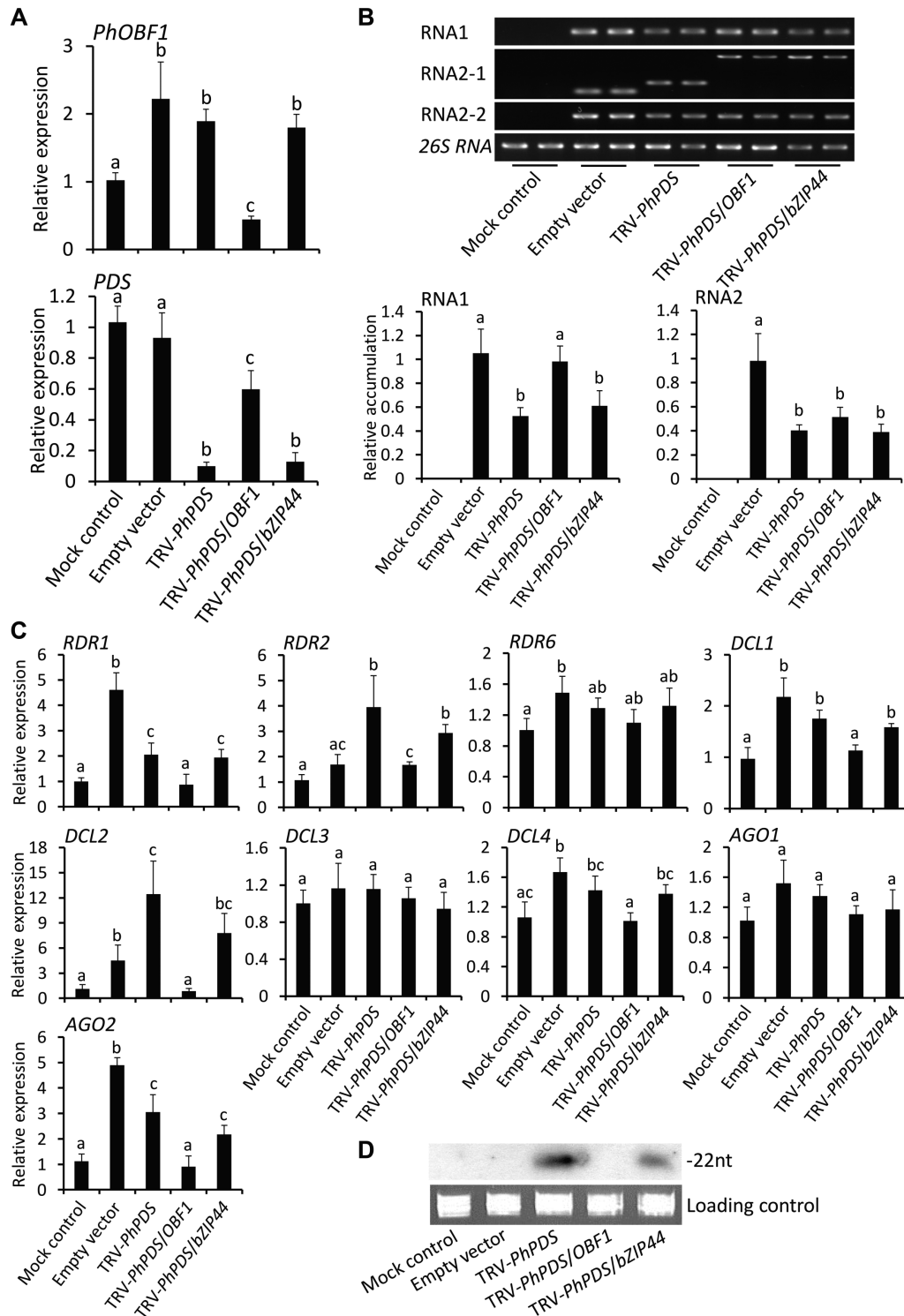


Fig. 3. Expression of *PhOBF1*, *PDS*, and RNA silencing-related genes and accumulation of TRV and siRNAs in the leaves of agro-infiltrated plants. (A) Quantitative real-time PCR analysis of *PhOBF1* and *PDS* transcript levels in uppermost leaves of plants at 3 weeks post-inoculation (wpi) with *Agrobacterium* bearing a TRV empty vector, TRV-PhPDS, TRV-PhPDS/OBF1, and TRV-PhPDS/bZIP44 constructs. Non-transformed *Agrobacterium* was used as mock control. Transcript abundances were standardized to 26S rRNA. (B) Semi-quantitative RT-PCR and quantitative real-time PCR analysis of TRV RNA1 and RNA2 (RNA2-1, -2) accumulation levels in uppermost leaves of plants at 3 wpi. Primers for RNA2-1 were designed based on the region outside of multiple cloning sites (MCS) in the vector and resulted product sizes were dependent on the inserted fragments of *PDS*, *PhOBF1/PDS*, and *PhOBF1/bZIP44*, while RNA2-2 targets the region upstream of MCS and produced the same sizes of products. (C) Quantitative real-time PCR analysis of transcript levels of RNA silencing-related genes, including *RDR1*, *RDR2*, *RDR6*, *DCL1*, *DCL2*, *DCL3*, *DCL4*, *AGO1*, and *AGO2*, in uppermost leaves of plants at 3 wpi. 26S rRNA was used as internal control. (D) Northern-blot analysis of TRV-PhPDS-derived siRNA levels in uppermost leaves of plants at 3 wpi. ³²P-labeled oligonucleotide probes correspond to *PDS* insert sequence. Ethidium bromide-stained 5S rRNA is indicated as a loading control. Error bars represent standard error of the mean from three biological replicates. Different letters indicate statistical significance as calculated by Duncan's multiple range test at $P < 0.05$.

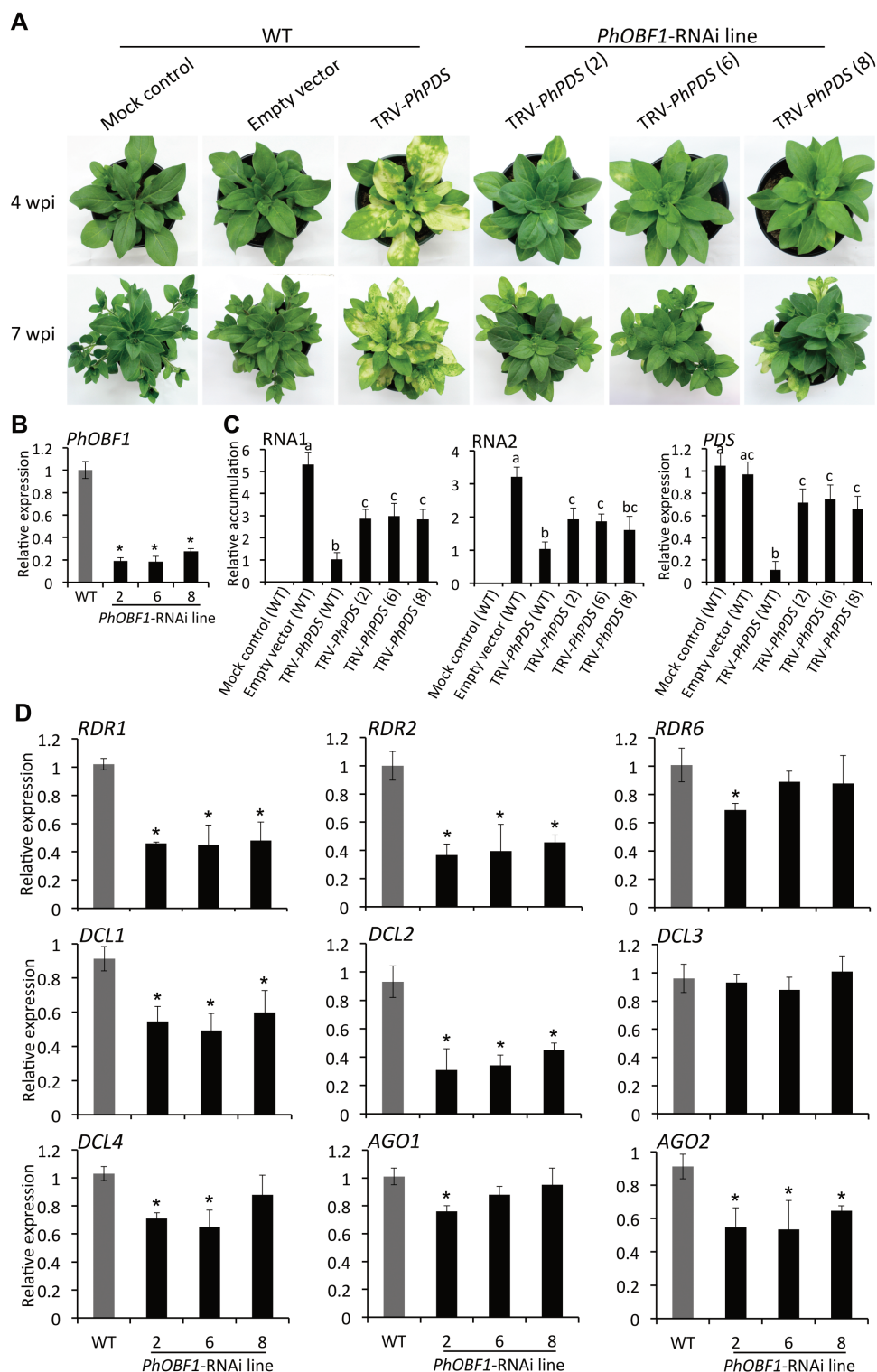


Fig. 4. Impairment of leaf photobleaching phenotype of *PDS* silencing in *PhERF2*-RNAi lines inoculated with *Agrobacterium* bearing TRV-*PhPDS*. (A) Representative phenotypes of WT and *PhOBF1*-RNAi lines (2, 6 and 8) inoculated with non-transformed *Agrobacterium* (mock control), or *Agrobacterium* bearing a TRV empty vector and TRV-*PhPDS* construct. Photographs were taken at 4 and 7 weeks post-inoculation (wpi). (B) Quantitative real-time PCR analysis of transcript abundances of *PhOBF1* in uppermost leaves of 4-week-old WT and *PhOBF1*-RNAi lines (2, 6 and 8). Expression levels were normalized to *26S rRNA*. (C) Quantitative real-time PCR analysis of TRV (RNA1 and RNA2) accumulation and *PDS* transcript levels in uppermost leaves of WT and *PhOBF1*-RNAi lines (2, 6 and 8) at 4 wpi. Accumulation and transcript levels were standardized to *26S rRNA*. (D) Quantitative real-time PCR analysis of transcript abundances of RNA silencing-related genes, including *RDR1*, *RDR2*, *RDR6*, *DCL1*, *DCL2*, *DCL3*, *DCL4*, *AGO1*, and *AGO2*, in uppermost leaves of 4-week-old WT and *PhOBF1*-RNAi lines (2, 6 and 8). *26S rRNA* was used as internal standard. Error bars represent standard error of the mean from three biological replicates. Significance of difference was calculated using Duncan's multiple range test ($P < 0.05$) and shown as asterisks or different letters.

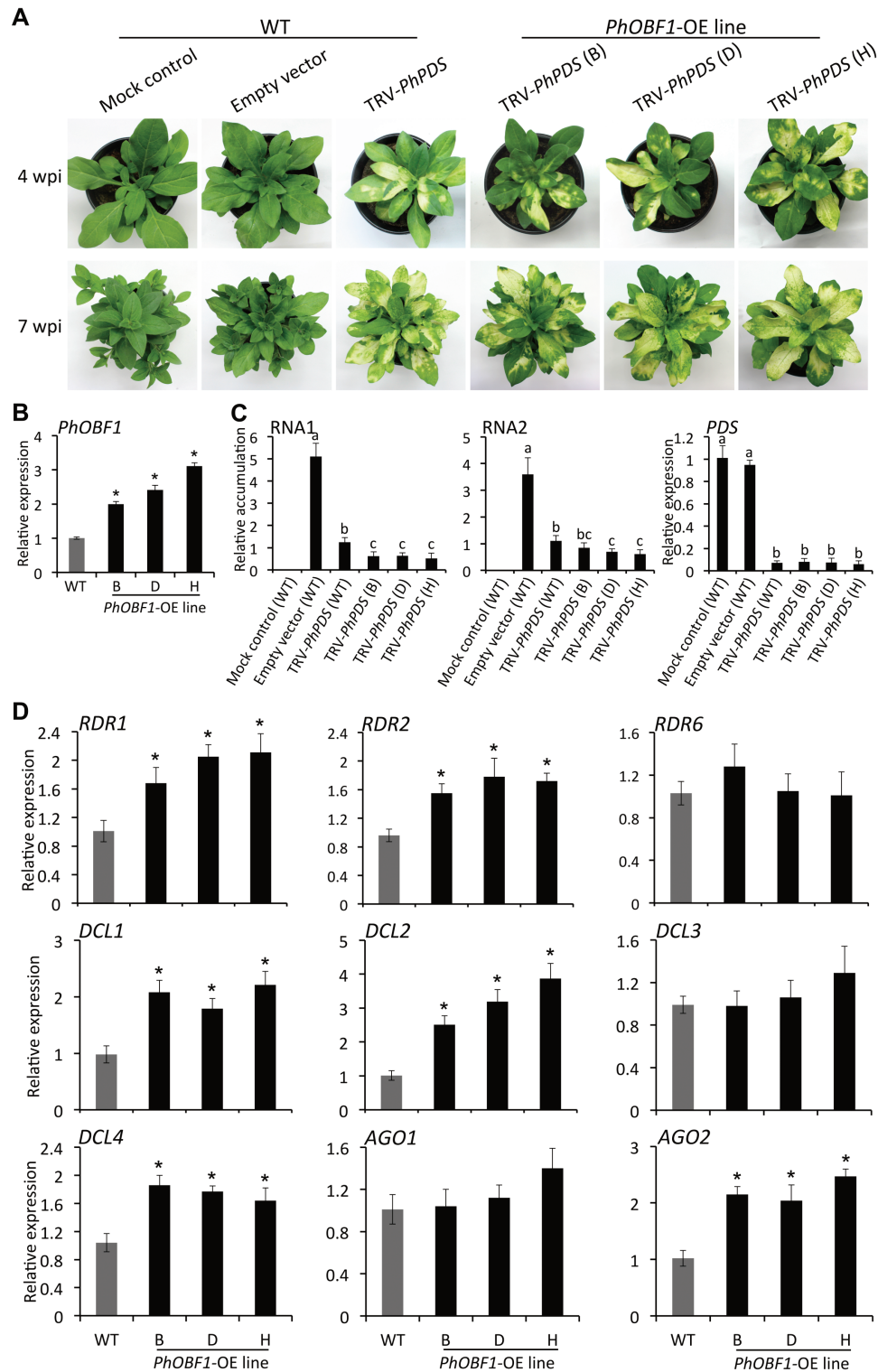


Fig. 5. Leaf photobleaching phenotype of *PDS* silencing in *PhOBF1*-overexpressing lines inoculated with *Agrobacterium* bearing TRV-*PhPDS*. (A) Representative phenotypes of WT and *PhOBF1*-overexpressing (OE) lines (B, D and H) inoculated with *Agrobacterium* bearing no TRV vector (mock control), or a TRV empty vector and TRV-*PhPDS* construct. Photographs were taken at 4 and 7 weeks post-inoculation (wpi). (B) Quantitative real-time PCR analysis of expression levels of *PhOBF1* in the leaves of WT and *PhOBF1*-OE lines (B, D and H). Samples were harvested from uppermost leaves of 4-week-old plants. *26S rRNA* was used as normalization control. (C) Quantitative real-time PCR analysis of TRV (RNA1 and RNA2) accumulation and *PDS* transcript abundances in uppermost leaves of WT and *PhOBF1*-OE lines (B, D and H) 4 wpi. *26S rRNA* was used as internal control. (D) Quantitative real-time PCR analysis of transcript abundances of RNA silencing-related genes, including *RDR1*, *RDR2*, *RDR6*, *DCL1*, *DCL2*, *DCL3*, *DCL4*, *AGO1*, and *AGO2*, in uppermost leaves of 4-week-old WT and *PhOBF1*-OE lines (B, D and H). Transcript levels were standardized to *26S rRNA*. Error bars represent standard error of the mean from three biological replicates. Asterisks or different letters indicate statistical significance using Duncan's multiple range test at $P < 0.05$.

under UV irradiation. At 6 dpi, the fluorescent area was visibly larger in *PhOBF1*-RNAi but smaller in *PhOBF1*-OE lines than in the control line (Fig. 6A, B). Furthermore, TRV empty vector was used for inoculation to observe virus symptom development in the transgenic and WT plants. Compared with WT, *PhOBF1*-RNAi lines exhibited a severer leaf mottling, chlorosis and curling symptoms at 4 wpi with

TRV, whereas the virus symptoms were considerably reduced in *PhOBF1*-OE lines (Fig. 6C). Consistent with that, higher accumulation levels of TRV RNA1 and RNA2 were found in *PhOBF1*-RNAi lines. On the other hand, lower accumulation levels were detected in the plants overexpressing *PhOBF1* than in WT plants (Fig. 6D and Supplementary Table S2). Furthermore, the WT plants inoculated with TMV developed

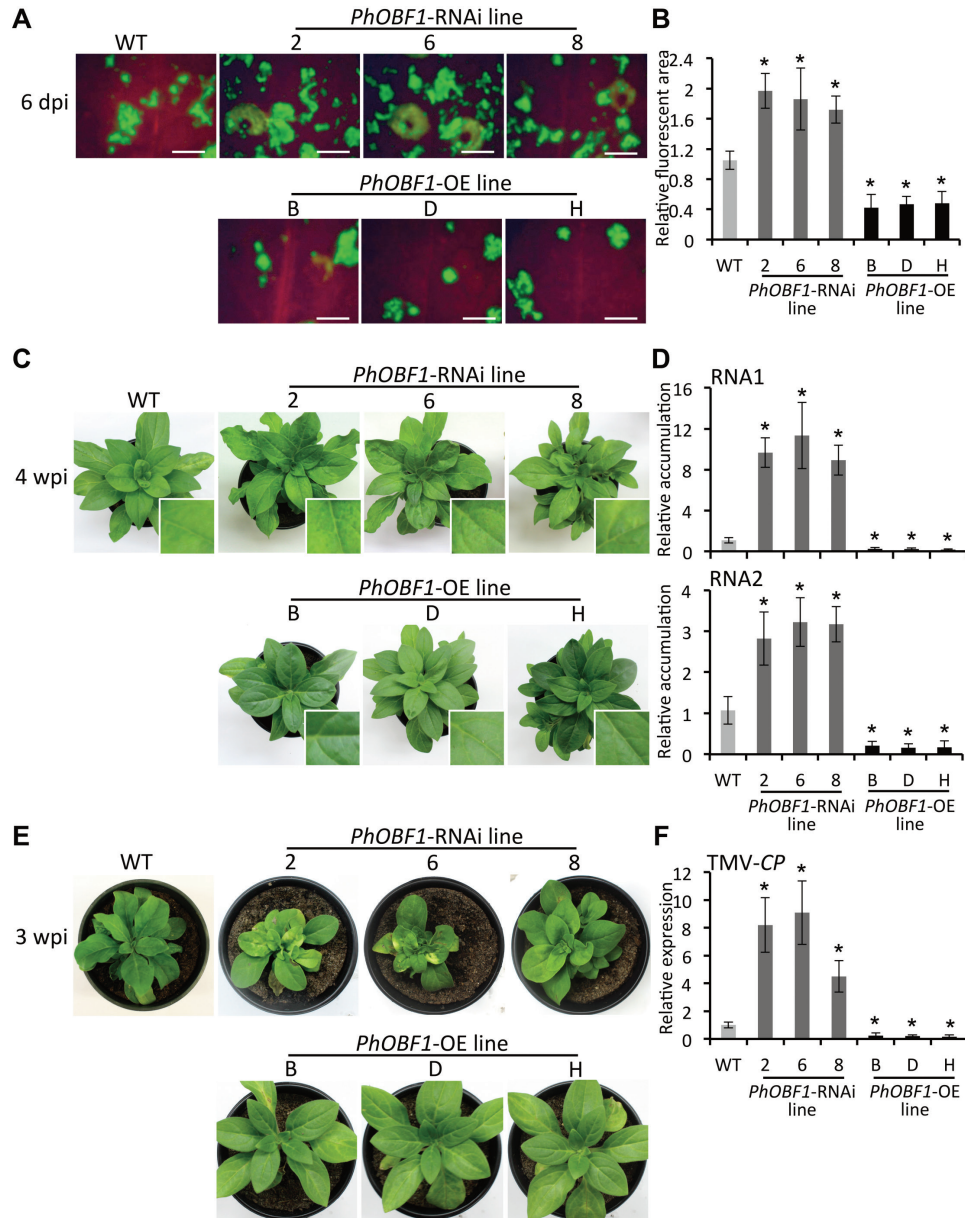


Fig. 6. Contribution of *PhOBF1* to petunia plant defense against TRV and TMV. GFP fluorescent foci (A) and relative fluorescent area (B) in inoculated leaves of WT, *PhOBF1*-RNAi (2, 6 and 8), and *PhOBF1*-overexpressing (OE) (B, D and H) lines at 6 days post-inoculation (dpi) with *Agrobacterium* bearing a TRV-GFP construct. Photographs were taken under UV light. Scale bars (A): 5 mm. Images of fluorescent area from three plants were analysed using Photoshop software. (C) Disease symptoms of WT, *PhOBF1*-RNAi (2, 6 and 8) and *PhOBF1*-OE (B, D and H) lines at 4 weeks post-inoculation (wpi) with *Agrobacterium* bearing a TRV empty vector. The insets are magnified views of viral symptoms in uppermost leaves infected with TRV. (D) Quantitative real-time PCR analysis of TRV (RNA1 and RNA2) accumulation levels in systemically infected (uppermost) leaves of WT, *PhOBF1*-RNAi (2, 6 and 8), and *PhOBF1*-OE (B, D and H) lines at 4 wpi. Transcript abundances were normalized to 26S *rRNA*. (E) Disease symptoms of WT, *PhOBF1*-RNAi (2, 6 and 8), and *PhOBF1*-OE (B, D and H) lines at 3 wpi with TMV. (F) Quantitative real-time PCR analysis of transcript levels of TMV-CP, encoding TMV coat protein, in systemically infected (uppermost) leaves of WT, *PhOBF1*-RNAi (2, 6 and 8), and *PhOBF1*-OE (B, D and H) lines at 3 wpi. 26S *rRNA* was used as an internal control. Error bars represent standard error of the mean from three biological replicates. Asterisks denote statistical significance as determined by Duncan's multiple range test at $P < 0.05$.

a symptom shown as slightly mottled and curled leaves, while leaf yellowing, necrosis, and dwarfing were observed in *PhOBFI*-RNAi lines. A much milder virus symptom was observed in *PhOBFI*-OE lines than in WT plants (Fig. 6E). At 3 wpi, *PhOBFI*-RNAi lines accumulated more transcripts of TMV-CP, encoding coat protein of TMV, but fewer TMV-CP transcripts were detected in *PhOBFI*-OE lines than in the control line (Fig. 6F and Supplementary Table S2).

PhOBFI modulates the biosynthesis of SA

Since the latest evidence suggests that transcripts of *RDR1*, *RDR2*, *DCL1*, and *DCL2* are up-regulated in tomato plants following CEVd, ToMV infection, and SA treatment (Campos *et al.*, 2014), we decided to examine the expression profile of RNA silencing-related genes in petunia plants

treated with exogenous SA, and to measure the free SA, SAG, and phenylalanine contents in WT and transgenic plants. SA treatment resulted in a dramatic induction of *RDR1*, *RDR2*, *DCL1*, *DCL2*, *DCL4*, and *AGO2* transcripts in petunia (Supplementary Fig. S4). Importantly, concentrations of free SA and conjugated SA were significantly reduced in *PhOBFI*-RNAi lines, but increased in *PhOBFI*-OE lines, compared with WT (Fig. 7A). Transgenic lines also showed similar alteration in concentrations of phenylalanine (Fig. 7B). Furthermore, we determined transcript abundances of the core genes in the shikimate and phenylpropanoid pathways that are associated with these biochemical changes. We found that transcript abundances of genes such as 3-deoxy-*d*-arabino-heptulosonate-7-phosphate synthase (*DAHPS*), shikimate kinase (*SK1*), 5-enolpyruvylshikimate 3-phosphate synthase (*EPSPS*), chorismate synthase (*CS*), chorismate mutase 1 (*CM1*),

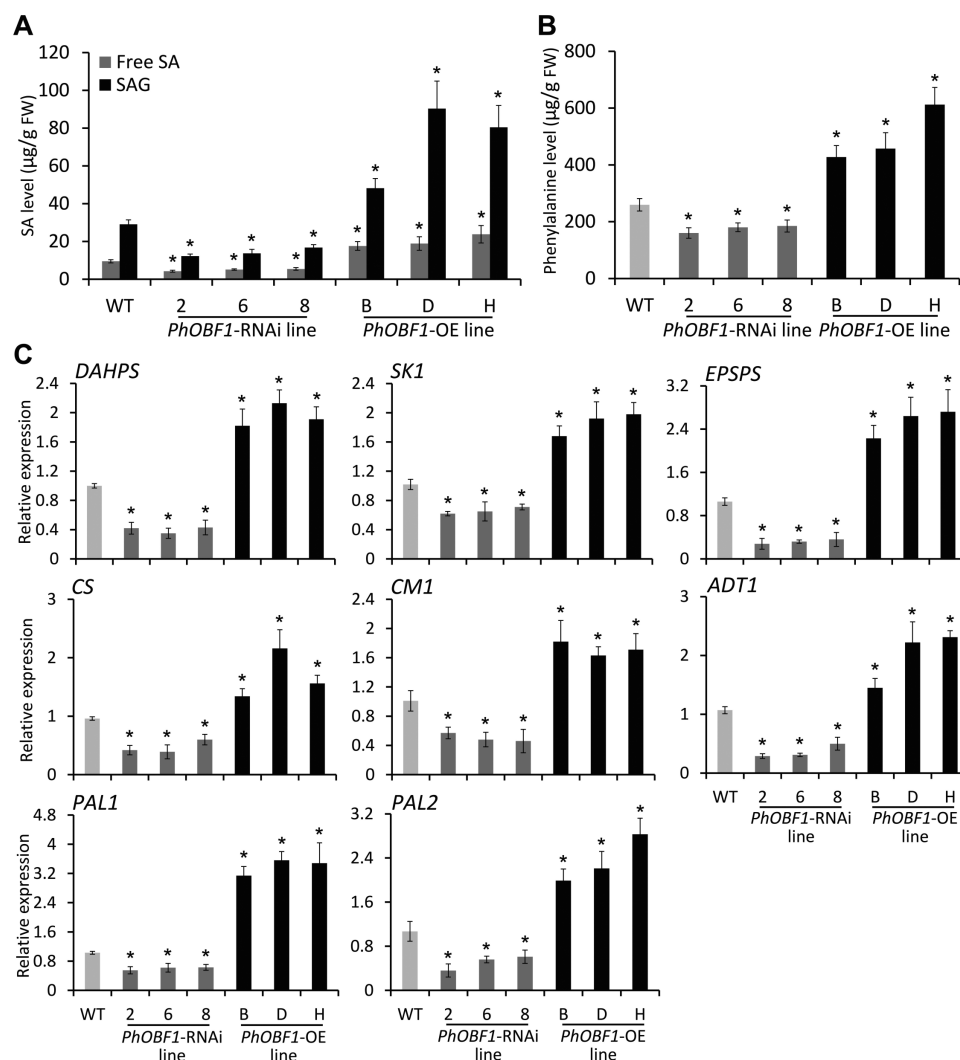


Fig. 7. Involvement of *PhOBFI* in the biosynthesis of salicylic acid. (A, B) Free SA, SA glucoside (SAG), and phenylalanine levels in the leaves of WT, *PhOBFI*-RNAi (2, 6 and 8), and *PhOBFI*-overexpressing (OE) (B, D and H) lines. Samples were harvested from all the leaves of 4-week-old WT and transgenic seedlings. (C) Quantitative real-time PCR analysis of transcript abundances of genes, including *DAHPS*, *SK1*, *EPSPS*, *CS*, *CM1*, *ADT1*, *PAL1*, and *PAL2*, in the shikimate and phenylpropanoid pathways in the leaves of WT, *PhOBFI*-RNAi (2, 6 and 8), and *PhOBFI*-OE (B, D and H) lines. Samples were harvested from the uppermost leaves of 4-week-old WT and transgenic seedlings. Expression levels were normalized to 26S *rRNA*. Error bars represent standard error of the mean from three biological replicates. Asterisks indicate statistical significance using Duncan's multiple range test at $P < 0.05$.

arogenate dehydratase 1 (*ADT1*), *PAL1*, and *PAL2* were significantly down-regulated in *PhOBF1*-RNAi lines, but up-regulated in *PhOBF1*-OE lines (Fig. 7C). These results suggested that *PhOBF1* may play important roles in the regulation of the RNA silencing pathway through biosynthesis of the hormone SA.

Discussion

In this study, our data suggest that the ocs element binding factor *PhOBF1* positively affects TRV-induced RNA silencing efficiency via the SA biosynthesis pathway (Fig. 8). OBF proteins bind to a class of DNA promoter sequences known as ocs elements or ACGT elements, which are essential for expression of bacterial and viral pathogen genes (Katagiri and Chua, 1992), and genes involved in the plant defense response (Ellis *et al.*, 1993; Chen and Singh, 1999). OBFs belong to a specific group of the bZIP transcription factor family in plants. A total of 75 members of the bZIP family have been identified in Arabidopsis (Jakoby *et al.*, 2002). The bZIP transcription factors induce the expression of genes whose promoter regions commonly share a core ACGT element, such as the G-box motif (CACGTG) (Hanson *et al.*, 2008). They participate in a variety of plant-specific processes, including pathogen resistance, stress response, light signaling, seed maturation and germination, and flower development (Jakoby *et al.*, 2002; Nijhawan *et al.*, 2008).

We have been investigating the role of regulatory genes, differentially expressed during petunia flower development, in the control of the corolla senescence process (Wang *et al.*, 2013). We employed the TRV-based VIGS method to silence these candidate genes, including *bZIPs*, to functionally study flower senescence-associated genes (Chang *et al.*, 2014; Yin *et al.*, 2015). When inoculated with TRV construct carrying *PhOBF1* and reporter gene (*PDS* or *CHS*) fragments,

the purple-flower petunia cultivar plants were incapable of developing the *PDS*- or *CHS*-silenced white leaves or flowers throughout the entire growth period (Fig. 2A, B), suggesting a dramatic reduction in VIGS efficiency. *PhOBF1* transcripts were partially down-regulated in the leaves from TRV-*PhPDS/OBF1*-infected plants, in which a reduction by approximately 40% in *PDS* levels occurred, compared with up to 90% reduction in *PDS* levels in photobleached leaves in the control (Fig. 3A). These data led us to hypothesize that *PhOBF1* probably functions as an important transcriptional regulator of antiviral RNA silencing.

RNA silencing triggered by virus dsRNA requires a few key components such as RDRs, DCLs and AGOs in plants (Costa *et al.*, 2013; Kasai *et al.*, 2013). Our data showed that the abundances of some RNA silencing-related genes, including *RDR1*, *RDR2*, *DCL1*, *DCL2*, *DCL4*, and *AGO2*, were decreased in the *PhOBF1*-silenced plants (Figs 3C and 4D) or increased in the *PhOBF1*-overexpressing transgenic plants (Fig. 5D). It is quite likely that *PhOBF1* contributes to the RNA silencing response by modulating the transcription of these genes.

RNA silencing serves as one type of antiviral mechanism, and exerts virus-derived siRNAs (vsiRNAs) as guides to target endogenous mRNA and simultaneously viral RNA (Ma *et al.*, 2015). Interference with the RNA silencing mechanism causes an impairment of resistance to diverse viruses. Many studies have been performed to examine the impact of key genes in the silencing complex on virus resistance. For example, mutation in the *DCL* genes results in more susceptibility to TCV and CMV (Bouché *et al.*, 2006), TRV (Donaire *et al.*, 2008), TMV (Lewsey and Carr, 2009), TuMV (Garcia-Ruiz *et al.*, 2010), and PVX (Andika *et al.*, 2015). A novel argonaute protein, AGO18, has been identified as conferring a broad-spectrum virus resistance in rice (Wu *et al.*, 2015). Given *PhOBF1*'s importance in RNA silencing, it is expected that *PhOBF1* is highly likely to be involved in plant resistance against a wide range of viral pathogens. Our findings of the compromised and enhanced resistance to TRV and TMV infections in *PhOBF1*-silenced and -overexpressing transgenic lines of petunia, respectively (Fig. 6), support this notion, and further prove the hypothesis that *PhOBF1* plays a pivotal role in the antiviral RNA silencing process. Moreover, we observed quite strong effects on VIGS silencing of reporter genes (*PDS* or *CHS*) and antiviral responses given the moderate down-regulation or overexpression of *PhOBF1*. The altered transcripts of multiple RNA silencing-related genes by *PhOBF1* probably contribute to these strong effects. *DCLs* and *AGOs* play different roles in antiviral RNA silencing, and the mutant lines *ago1-27* and *dcl2/dcl3/dcl4* infected with TRV-*PhPDS* show impaired leaf photobleaching and increased TRV accumulation (Ma *et al.*, 2015). But it appears that those single or triple mutants have a relatively mild impact on gene silencing and antiviral defense compared with the *PhOBF1* silencing or overexpression. As a powerful transcription factor, *PhOBF1* may greatly affect the antiviral RNA silencing process by regulating other critical factors, such as SA.

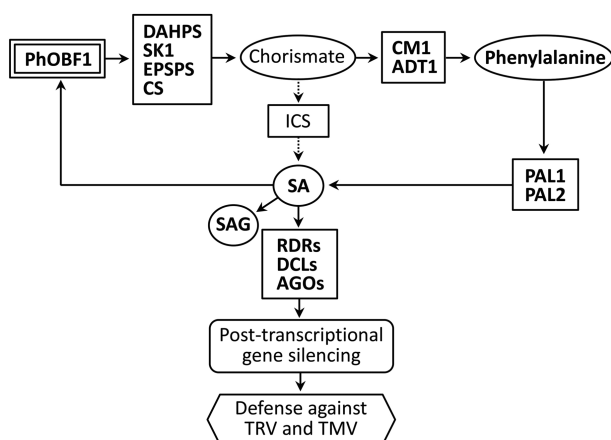


Fig. 8. A proposed model for *PhOBF1* function in antiviral RNA silencing. *PhOBF1* positively regulates the genes in the shikimate and phenylpropanoid pathways, as well as phenylalanine and SA accumulation. Ultimately, *PhOBF1* contributes to extensive resistance to TRV and TMV through SA-mediated post-transcriptional gene silencing. Solid arrows indicate well-described relationships, and dotted arrows indicate undescribed steps in this work. The SA, SAG, phenylalanine, and related genes analysed in *PhOBF1*-RNAi and -OE lines are shown in bold.

Many pieces of evidence have revealed a close association between antiviral RNA silencing and the plant endogenous hormone SA. Both ToMV and CEVd infections promote the accumulation of SA (Bellés *et al.*, 1999), as well as transcript levels of a number of *RDR* and *DCL* genes (Campos *et al.*, 2014). Exogenous SA treatment reduces the infection caused by *Alfalfa mosaic virus* (AIMV) (Van Huijsduijnen *et al.*, 1986), TMV (Chivasa *et al.*, 1997; Murphy and Carr, 2002; Shang *et al.*, 2011), CMV and TCV (Shang *et al.*, 2011), and PVX (Falcioni *et al.*, 2014). Degradation of SA in tobacco results in a reduced accumulation of virus-derived siRNAs and enhanced virus multiplication (Alamillo *et al.*, 2006). Moreover, exogenous SA treatment not only increases the levels of *RDR1* in Arabidopsis or tobacco (Yang *et al.*, 2004; Quilis *et al.*, 2008), but also *RDR2*, *DCL1*, and *DCL2* transcript abundances in tomato (Campos *et al.*, 2014). Our observations of significantly increased expression levels of *RDR1*, *RDR2*, *DCL1*, *DCL2*, *DCL4*, and *AGO2* in petunia following treatment with SA (Supplementary Fig. S4) are consistent with these findings. In addition, we found that the impaired and recovered *PDS*-silenced leaf photobleaching phenotypes in *PhOBF1*-silenced and -overexpressing petunias were accompanied by reduced and increased endogenous SA levels, respectively (Fig. 7A). It seems possible that SA serves as an intermediate signal linking PhOBF1 with the antiviral RNA silencing pathway. Future studies will determine if exogenous SA treatment can recover the impaired *PDS*-silenced leaf photobleaching or *CHS*-silenced white-corollas phenotype in *PhOBF1*-silenced petunia plants inoculated with TRV constructs carrying reporter genes (*PDS* or *CHS*).

SA biosynthesis involves the shikimate and phenylpropanoid pathways, which are controlled by some critical genes, such as *DAHPS*, *SKI*, *EPSPS*, *CS*, *CM1*, *ADT1*, *PAL1*, and *PAL2*. Apart from SA content, we found that PhOBF1 silencing and overexpression led to down-regulation and up-regulation of these genes, respectively (Fig. 7C). Interestingly, silencing of R2R3-MYB-like transcription factors, *ODO1* (Verdonk *et al.*, 2005), *EOBI* and *EOBII* (Spitzer-Rimon *et al.*, 2012), also results in reduction of a set of genes transcripts in the shikimate and phenylpropanoid pathways. *ODO1*, transcriptionally regulated by *EOBI* and *EOBII* (Spitzer-Rimon *et al.*, 2012), is involved in floral fragrance production of petunia, and its suppression causes a decreased level of methyl salicylate (Verdonk *et al.*, 2005). It appears likely that one of these three MYB-like genes might be a crucial target of PhOBF1 for the SA-mediated RNA silencing mechanism. However, we found that the petunia plants inoculated with TRV-*PhCHS/ODO1* in the VIGS assay showed the *CHS*-silenced white-corollas phenotype (data not shown), suggesting that PhOBF1 is unlikely to regulate the SA-mediated antiviral RNA silencing system by activating downstream *ODO1* expression. The involvement of PhOBF1 in floral scent biosynthesis requires further examination in the future.

It should be mentioned that TRV 16 kDa (16K) protein, encoded by genomic RNA1, functions as a suppressor of RNA silencing. However, unlike the strong silencing suppressors CMV 2b (Goto *et al.*, 2007) and Tombusvirus P19

(Lakatos *et al.*, 2004), TRV 16K acts as a weak suppressor that transiently blocks local RNA silencing and enhances viral RNA accumulation early (Martínez-Priego *et al.*, 2008). In this study, we mainly focused on the silencing phenotypes in systemic leaves or flowers infected with various TRV constructs. It seems likely that the silencing of endogenous genes and antiviral defenses in inoculated leaves are more complex. In the early infection process, 16K suppressor may impose effects on PhOBF1-involved antiviral RNA silencing, and it remains unclear whether these effects can lead to the changes of final responses in systemically infected tissues. Furthermore, a possible relationship between PhOBF1 and TRV 16K suppressor should be explored in future work.

We are interested in the role of PhOBF1 in the regulation of flower senescence. Ethylene treatment increased the transcripts of *PhOBF1* (Fig. 1D). Its transcript levels were also up-regulated at various developmental stages of petunia corollas (Supplementary Fig. S5). Our analysis of flower longevity revealed that silencing of *PhOBF1* accelerated flower senescence and its overexpression extended flower longevity (Supplementary Table S3). Furthermore, both ABA and GA₃ treatments increased the expression levels of *PhOBF1* (Fig. 1D). The crosstalk between ethylene and ABA (Chang *et al.*, 2014) or GA₃ (Yin *et al.*, 2015) during flower senescence has been discussed in petunia. More studies are required to clarify the role of PhOBF1 in the regulation of petunia flower senescence. Additionally, the role of PhOBF1 in plant growth and development should be further investigated, because we found that down-regulation of *PhOBF1* resulted in increased plant height and reduced stem diameter, while overexpression of *PhOBF1* caused slightly smaller and thicker leaves (data not shown).

It is worth mentioning that PhERF2, an ERF transcription factor we previously reported, plays a quite similar role in antiviral RNA silencing to PhOBF1. *PhERF2* silencing also substantially impaired the *PDS*-silenced leaf photobleaching phenotype and *PhERF2* overexpression restored it (Sun *et al.*, 2016). The same involvements of PhOBF1 and PhERF2 in resistance to TRV were found. Thus, we hypothesize that a close association between PhOBF1 and PhERF2 probably occurs. In Arabidopsis, OBF4 interacts with an ethylene-responsive element binding factor AtEBP and may collaboratively contribute to the plant defense response (Büttner and Singh, 1997). However, we did not find altered *PhERF2* expression in *PhOBF1*-silenced and -overexpressing lines, or altered *PhOBF1* expression in *PhERF2* transgenic lines (data not shown). *PhOBF1* and *PhERF2* affected transcript levels of different RNA silencing-related genes, and for example, *PhOBF1* rather than *PhERF2* affected expression levels of *RDR1*, *DCL1*, and *DCL4*. Moreover, PhOBF1, not PhERF2, plays a role in the regulation of petunia flower senescence. One explanation is that they perhaps regulate TRV-induced RNA silencing through two distinct pathways. ERF proteins specifically bind to the GCC box, which commonly presents in the promoter of downstream defensive genes of the ethylene signaling pathway (Ohme-Takagi and Shinshi, 1995). It seems likely that PhOBF1 and PhERF2 may be a positive regulator in the SA biosynthesis pathway and ethylene signaling pathway, respectively.

Our data demonstrate that PhOBF1 plays an important role in antiviral RNA silencing. The positive regulation of PhOBF1 in the TRV-induced gene silencing process via SA may provide a feasible approach to improve the efficiency of the TRV-based VIGS system, through a transient overexpression of *PhOBF1* or its homologs, or an appropriate application of exogenous SA. Further confirmation should be sought for whether PhOBF1 also plays a regulatory role in other virus-based VIGS systems besides TRV. It is noteworthy that abiotic stresses, such as salt, drought, oxidation and low temperature, induce the expression of a number of RNA silencing-related genes in tomato (Bai *et al.*, 2012). We also found that low temperature and dehydration treatments increased the transcript levels of *PhOBF1* (Fig. 1C). The existing evidence supports that low temperature and low humidity enhance TRV-induced gene silencing efficiency in tomato (Fu *et al.*, 2006). The effects of these abiotic stresses on the RNA silencing response still require more study in the future.

Supplementary data

Supplementary data are available at *JXB* online.

Fig. S1. Petunia *PhOBF1* cDNA and deduced amino acid sequence analysis.

Fig. S2. Expression of *PhOBF1* in various tissues of petunia plant.

Fig. S3. Failed development of leaf photobleaching and white-corollas phenotypes in petunia plants inoculated with a *PhPDS/CHS/OBF1* tandem TRV construct.

Fig. S4. Induction of RNA silencing-related genes in petunia leaves treated with salicylic acid.

Fig. S5. Induction of *PhOBF1* expression during petunia flower senescence.

Table S1. Primers used for semi-quantitative RT-PCR and quantitative real-time PCR.

Table S2. The numerical data for relative accumulation or expression levels of TRV RNAs and TMV-CP in WT, *PhOBF1*-RNAi and *PhOBF1*-overexpressing lines infected with TRV empty vector and TMV, respectively.

Table S3. The longevity of attached flowers from WT, *PhOBF1*-RNAi and *PhOBF1*-overexpressing lines.

Acknowledgements

We thank Bryce Falk and Raja Sekhar Nandety for experimental assistance in northern blot analysis. We are grateful to Lee Ann Richmond for operation of the laboratory instruments. We thank Weixing Shan for kindly providing the TMV strains. We also thank the anonymous reviewers for their invaluable suggestions for further improvement of the manuscript. This study was partially funded by United States Department of Agriculture (USDA) CRIS project 5306-21000-019-00D.

References

- Alamillo JM, Saénz P, García JA. 2006. Salicylic acid-mediated and RNA-silencing defense mechanisms cooperate in the restriction of systemic spread of plum pox virus in tobacco. *The Plant Journal* **48**, 217–227.
- Alvarado VY, Scholthof HB. 2011. AGO2: A new argonaute compromising plant virus accumulation. *Frontiers in Plant Science* **2**, 112.

- Andika IB, Maruyama K, Sun L, Kondo H, Tamada T, Suzuki N. 2015. Differential contributions of plant Dicer-like proteins to antiviral defences against *Potato virus X* in leaves and roots. *The Plant Journal* **81**, 781–793.
- Axtell MJ. 2013. Classification and comparison of small RNAs from plants. *Annual Review of Plant Biology* **64**, 137–159.
- Bai M, Yang GS, Chen WT, Mao ZC, Kang HX, Chen GH, Yang YH, Xie BY. 2012. Genome-wide identification of Dicer-like, Argonaute and RNA-dependent RNA polymerase gene families and their expression analyses in response to viral infection and abiotic stresses in *Solanum lycopersicum*. *Gene* **501**, 52–62.
- Bartel B, Bartel DP. 2003. MicroRNAs: at the root of plant development? *Plant Physiology* **132**, 709–717.
- Baumberger N, Baulcombe D. 2005. *Arabidopsis* Argonaute1 is an RNA Slicer that selectively recruits microRNAs and short interfering RNAs. *Proceedings of the National Academy of Sciences, USA* **102**, 11928–11933.
- Bellés JM, Garro R, Fayos J, Navarro P, Primo J, Conejero V. 1999. Gentisic acid as a pathogen-inducible signal, additional to salicylic acid for activation of plant defenses in tomato. *Molecular Plant-Microbe Interactions* **12**, 227–235.
- Bouché N, Laressergues D, Gasciolli V, Vaucheret H. 2006. An antagonistic function for *Arabidopsis* DCL2 in development and a new function for DCL4 in generating viral siRNAs. *The EMBO Journal* **25**, 3347–3356.
- Burch-Smith TM, Schiff M, Liu Y, Dinesh-Kumar SP. 2006. Efficient virus-induced gene silencing in *Arabidopsis*. *Plant Physiology* **142**, 21–27.
- Büttner M, Singh KB. 1997. *Arabidopsis thaliana* ethylene-responsive element binding protein (AtEBP), an ethylene-inducible, GCC box DNA-binding protein interacts with an ocs element binding protein. *Proceedings of the National Academy of Sciences, USA* **94**, 5961–5966.
- Campos L, Granell P, Tárraga S, López-Gresa P, Conejero V, Bellés JM, Rodrigo I, Lisón P. 2014. Salicylic acid and gentisic acid induce RNA silencing-related genes and plant resistance to RNA pathogens. *Plant Physiology and Biochemistry* **77**, 35–43.
- Chang X, Donnelly L, Sun D, Rao J, Reid MS, Jiang CZ. 2014. A Petunia homeodomain-leucine zipper protein, PhHD-Zip, plays an important role in flower senescence. *PLoS One* **9**, e88320.
- Chen JC, Jiang CZ, Gookin TE, Hunter DA, Clark DG, Reid MS. 2004. Chalcone synthase as a reporter in virus-induced gene silencing studies of flower senescence. *Plant Molecular Biology* **55**, 521–530.
- Chen W, Singh KB. 1999. The auxin, hydrogen peroxide and salicylic acid induced expression of the *Arabidopsis* GST6 promoter is mediated in part by an ocs element. *The Plant Journal* **19**, 667–677.
- Chivasa S, Murphy AM, Naylor M, Carr JP. 1997. Salicylic acid interferes with tobacco mosaic virus replication via a novel salicylhydroxamic acid-sensitive mechanism. *The Plant Cell* **9**, 547–557.
- Costa AT, Bravo JP, Makiyama RK, Nunes AV, Maia IG. 2013. Viral counter defense X antiviral immunity in plants: mechanisms for survival. In: Romanowski C, ed. *Current issues in molecular virology – Viral genetics and biotechnological applications*. Rijeka, Croatia: Intech, 251–285.
- Deleris A, Gallego-Bartolome J, Bao J, Kasschau KD, Carrington JC, Voinnet O. 2006. Hierarchical action and inhibition of plant Dicer-like proteins in antiviral defense. *Science* **313**, 68–71.
- D'Maris Amick Dempsey AC, Vlot MCW, Daniel FK. 2011. Salicylic acid biosynthesis and metabolism. *The Arabidopsis Book* **9**, e0156.
- Donaire L, Barajas D, Martínez-García B, Martínez-Priego L, Pagán I, Llave C. 2008. Structural and genetic requirements for the biogenesis of tobacco rattle virus-derived small interfering RNAs. *Journal of Virology* **82**, 5167–5177.
- Ellis JG, Tokuhisa JG, Llewellyn DJ, Bouchez D, Singh K, Dennis ES, Peacock WJ. 1993. Does the ocs-element occur as a functional component of the promoters of plant genes? *The Plant Journal* **4**, 433–443.
- Estrada-Melo AC, Ma C, Reid MS, Jiang CZ. 2015. Overexpression of an ABA biosynthesis gene using a stress-inducible promoter enhances drought resistance in petunia. *Horticulture Research* **2**, 15013.
- Falcioni T, Ferrio JP, Del Cueto AI, Giné J, Achón MÁ, Medina V. 2014. Effect of salicylic acid treatment on tomato plant physiology and tolerance to *Potato virus X* infection. *European Journal of Plant Pathology* **138**, 331–345.

- Fu DQ, Zhu BZ, Zhu HL, Zhang HX, Xie YH, Jiang WB, Zhao XD, Luo KB.** 2006. Enhancement of virus-induced gene silencing in tomato by low temperature and low humidity. *Molecules and Cells* **21**, 153–160.
- Garcia-Ruiz H, Takeda A, Chapman EJ, Sullivan CM, Fahlgren N, Brempelis KJ, Carrington JC.** 2010. *Arabidopsis* RNA-dependent RNA polymerases and dicer-like proteins in antiviral defense and small interfering RNA biogenesis during *Turnip Mosaic Virus* infection. *The Plant Cell* **22**, 481–496.
- Goto K, Kobori T, Kosaka Y, Natsuaki T, Masuta C.** 2007. Characterization of silencing suppressor 2b of cucumber mosaic virus based on examination of its small RNA-binding abilities. *Plant & Cell Physiology* **48**, 1050–1060.
- Gould B, Kramer EM.** 2007. Virus-induced gene silencing as a tool for functional analyses in the emerging model plant *Aquilegia* (columbine, Ranunculaceae). *Plant Methods* **3**, 6.
- Hanson J, Hanssen M, Wiese A, Hendriks MM, Smeekens S.** 2008. The sucrose regulated transcription factor bZIP11 affects amino acid metabolism by regulating the expression of *ASPARAGINE SYNTHETASE1* and *PROLINE DEHYDROGENASE2*. *The Plant Journal* **53**, 935–949.
- Harvey JJ, Lewsey MG, Patel K, Westwood J, Heimstädt S, Carr JP, Baulcombe DC.** 2011. An antiviral defense role of AGO2 in plants. *PLoS One* **6**, e14639.
- Hull R.** 2009. Mechanical inoculation of plant viruses. *Current Protocols in Microbiology* **16B.6**, doi:10.1002/9780471729259.mc16b06s13.
- Jakoby M, Weissshaar B, Dröge-Laser W, Vicente-Carbajosa J, Tiedemann J, Kroj T, Parcy F; bZIP Research Group.** 2002. bZIP transcription factors in *Arabidopsis*. *Trends in Plant Science* **7**, 106–111.
- Janzik I, Preiskowski S, Kneifel H.** 2005. Ozone has dramatic effects on the regulation of the prechormate pathway in tobacco (*Nicotiana tabacum* L. cv. Bel W3). *Planta* **223**, 20–27.
- Jaubert M, Bhattacharjee S, Mello AF, Perry KL, Moffett P.** 2011. ARGONAUTE2 mediates RNA-silencing antiviral defenses against *Potato virus X* in *Arabidopsis*. *Plant Physiology* **156**, 1556–1564.
- Ji LH, Ding SW.** 2001. The suppressor of transgene RNA silencing encoded by Cucumber mosaic virus interferes with salicylic acid-mediated virus resistance. *Molecular Plant-Microbe Interactions* **14**, 715–724.
- Jiang CZ, Chen JC, Reid MS.** 2011. Virus-induced gene silencing in ornamental plants. In: Kodama H, Komamine A, eds. *RNAi and plant gene function analysis*. New York: Humana Press, 81–96.
- Kasai M, Matsumura H, Yoshida K, Terauchi R, Taneda A, Kanazawa A.** 2013. Deep sequencing uncovers commonality in small RNA profiles between transgene-induced and naturally occurring RNA silencing of chalcone synthase-A gene in petunia. *BMC Genomics* **14**, 63.
- Katagiri F, Chua NH.** 1992. Plant transcription factors: present knowledge and future challenges. *Trends in Genetics* **8**, 22–27.
- Kumar D, Klessig DF.** 2003. High-affinity salicylic acid-binding protein 2 is required for plant innate immunity and has salicylic acid-stimulated lipase activity. *Proceedings of the National Academy of Sciences, USA* **100**, 16101–16106.
- Kusano T, Berberich T, Harada M, Suzuki N, Sugawara K.** 1995. A maize DNA-binding factor with a bZIP motif is induced by low temperature. *Molecular & General Genetics* **248**, 507–517.
- Kusano T, Sugawara K, Harada M, Berberich T.** 1998. Molecular cloning and partial characterization of a tobacco cDNA encoding a small bZIP protein. *Biochimica et Biophysica Acta* **1395**, 171–175.
- Lakatos L, Szittyá G, Silhavy D, Burgyn J.** 2004. Molecular mechanism of RNA silencing suppression mediated by p19 protein of tombusviruses. *The EMBO Journal* **23**, 876–884.
- Lee DH, Choi HW, Hwang BK.** 2011. The pepper E3 ubiquitin ligase RING1 gene, CaRING1, is required for cell death and the salicylic acid-dependent defense response. *Plant Physiology* **156**, 2011–2025.
- Lewsey MG, Carr JP.** 2009. Effects of DICER-like proteins 2, 3 and 4 on cucumber mosaic virus and tobacco mosaic virus infections in salicylic acid-treated plants. *The Journal of General Virology* **90**, 3010–3014.
- Liang YC, Reid MS, Jiang CZ.** 2014. Controlling plant architecture by manipulation of gibberellic acid signalling in petunia. *Horticulture Research* **1**, 14061.
- Ma J, Hanssen M, Lundgren K, et al.** 2011. The sucrose-regulated *Arabidopsis* transcription factor bZIP11 reprograms metabolism and regulates trehalose metabolism. *The New Phytologist* **191**, 733–745.
- Ma X, Nicole MC, Metegnier LV, Hong N, Wang G, Moffett P.** 2015. Different roles for RNA silencing and RNA processing components in virus recovery and virus-induced gene silencing in plants. *Journal of Experimental Botany* **66**, 919–932.
- Malamy J, Carr JP, Klessig DF, Raskin I.** 1990. Salicylic acid: a likely endogenous signal in the resistance response of tobacco to viral infection. *Science* **250**, 1002–1004.
- Martínez-Priego L, Donaire L, Barajas D, Llave C.** 2008. Silencing suppressor activity of the *Tobacco rattle virus*-encoded 16-kDa protein and interference with endogenous small RNA-guided regulatory pathways. *Virology* **376**, 346–356.
- Molnar A, Melnyk CW, Bassett A, Hardcastle TJ, Dunn R, Baulcombe DC.** 2010. Small silencing RNAs in plants are mobile and direct epigenetic modification in recipient cells. *Science* **328**, 872–875.
- Murphy AM, Carr JP.** 2002. Salicylic acid has cell-specific effects on tobacco mosaic virus replication and cell-to-cell movement. *Plant Physiology* **128**, 552–563.
- Nijhawan A, Jain M, Tyagi AK, Khurana JP.** 2008. Genomic survey and gene expression analysis of the basic leucine zipper transcription factor family in rice. *Plant Physiology* **146**, 333–350.
- Ohme-Takagi M, Shinshi H.** 1995. Ethylene-inducible DNA binding proteins that interact with an ethylene-responsive element. *The Plant Cell* **7**, 173–182.
- Qu F, Ye X, Morris TJ.** 2008. *Arabidopsis* DRB4, AGO1, AGO7, and RDR6 participate in a DCL4-initiated antiviral RNA silencing pathway negatively regulated by DCL1. *Proceedings of the National Academy of Sciences, USA* **105**, 14732–14737.
- Quilis J, Peñas G, Messegue J, Brugidou C, San Segundo B.** 2008. The *Arabidopsis* AtNPR1 inversely modulates defense responses against fungal, bacterial, or viral pathogens while conferring hypersensitivity to abiotic stresses in transgenic rice. *Molecular Plant-Microbe Interactions* **21**, 1215–1231.
- Reid MS, Chen JC, Jiang CZ.** 2009. Virus-induced gene silencing for functional characterization of genes in petunia. In: Gerats T, Strommer J, eds. *Petunia*. Berlin Heidelberg: Springer, 381–394.
- Riechmann JL, Heard J, Martin G, et al.** 2000. *Arabidopsis* transcription factors: genome-wide comparative analysis among eukaryotes. *Science* **290**, 2105–2110.
- Rivas-San Vicente M, Plasencia J.** 2011. Salicylic acid beyond defence: its role in plant growth and development. *Journal of Experimental Botany* **62**, 3321–3338.
- Scholthof HB, Alvarado VY, Vega-Arrequin JC, Ciomperlik J, Odokonyero D, Brosseau C, Jaubert M, Zamora A, Moffett P.** 2011. Identification of an ARGONAUTE for antiviral RNA silencing in *Nicotiana benthamiana*. *Plant Physiology* **156**, 1548–1555.
- Schwach F, Vaistij FE, Jones L, Baulcombe DC.** 2005. An RNA-dependent RNA polymerase prevents meristem invasion by *Potato virus X* and is required for the activity but not the production of a systemic silencing signal. *Plant Physiology* **138**, 1842–1852.
- Shang J, Xi DH, Xu F, et al.** 2011. A broad-spectrum, efficient and nontransgenic approach to control plant viruses by application of salicylic acid and jasmonic acid. *Planta* **233**, 299–308.
- Shimizu H, Sato K, Berberich T, Miyazaki A, Ozaki R, Imai R, Kusano T.** 2005. LIP19, a basic region leucine zipper protein, is a Fos-like molecular switch in the cold signaling of rice plants. *Plant & Cell Physiology* **46**, 1623–1634.
- Spitzer-Rimon B, Farhi M, Albo B, et al.** 2012. The R2R3-MYB-like regulatory factor EOBI, acting downstream of EOBI, regulates scent production by activating ODO1 and structural scent-related genes in petunia. *The Plant Cell* **24**, 5089–5105.
- Sun D, Nandety RS, Zhang Y, Reid MS, Niu L, Jiang CZ.** 2016. A petunia ethylene-responsive element binding factor, PhERF2, plays an important role in antiviral RNA silencing. *Journal of Experimental Botany* **67**, 3353–3365.
- Thalor SK, Berberich T, Lee SS, Yang SH, Zhu X, Imai R, Takahashi Y, Kusano T.** 2012. Dereglulation of sucrose-controlled translation of a bZIP-type transcription factor results in sucrose accumulation in leaves. *PLoS One* **7**, e33111.

- Tian J, Pei H, Zhang S, Chen J, Chen W, Yang R, Meng Y, You J, Gao J, Ma N.** 2014. TRV-GFP: a modified Tobacco rattle virus vector for efficient and visualizable analysis of gene function. *Journal of Experimental Botany* **65**, 311–322.
- Tzin V, Galili G.** 2010. The Biosynthetic pathways for shikimate and aromatic amino acids in *Arabidopsis thaliana*. *The Arabidopsis Book* **8**, e0132.
- Van Huijsduijnen RH, Alblas S, De Rijk R, Bol J.** 1986. Induction by salicylic acid of pathogenesis-related proteins and resistance to *Alfalfa mosaic virus* infection in various plant species. *Journal of General Virology* **67**, 2135–2143.
- Verdonk JC, Haring MA, van Tunen AJ, Schuurink RC.** 2005. ODORANT1 regulates fragrance biosynthesis in petunia flowers. *The Plant Cell* **17**, 1612–1624.
- Voinnet O.** 2009. Origin, biogenesis, and activity of plant microRNAs. *Cell* **136**, 669–687.
- Wang H, Stier G, Lin J, Liu G, Zhang Z, Chang Y, Reid MS, Jiang CZ.** 2013. Transcriptome changes associated with delayed flower senescence on transgenic petunia by inducing expression of *etr1-1*, a mutant ethylene receptor. *PLoS One* **8**, e65800.
- Wang JF, Zhou H, Chen YQ, Luo QJ, Qu LH.** 2004. Identification of 20 microRNAs from *Oryza sativa*. *Nucleic Acids Research* **32**, 1688–1695.
- Wang XB, Jovel J, Udornporn P, Wang Y, Wu Q, Li WX, Gasciolli V, Vaucheret H, Ding SW.** 2011. The 21-nucleotide, but not 22-nucleotide, viral secondary small interfering RNAs direct potent antiviral defense by two cooperative argonautes in *Arabidopsis thaliana*. *The Plant Cell* **23**, 1625–1638.
- Wang XB, Wu Q, Ito T, Cillo F, Li WX, Chen X, Yu JL, Ding SW.** 2010. RNAi-mediated viral immunity requires amplification of virus-derived siRNAs in *Arabidopsis thaliana*. *Proceedings of the National Academy of Sciences, USA* **107**, 484–489.
- Weiste C, Dröge-Laser W.** 2014. The *Arabidopsis* transcription factor bZIP11 activates auxin-mediated transcription by recruiting the histone acetylation machinery. *Nature Communications* **5**, 3883.
- Wiese A, Elzinga N, Wobbes B, Smeekens S.** 2004. A conserved upstream open reading frame mediates sucrose-induced repression of translation. *The Plant Cell* **16**, 1717–1729.
- Wu J, Yang Z, Wang Y, Zheng L, Ye R, Ji Y, Zhao S, Ji S, Liu R, Xu L.** 2015. Viral-inducible Argonaute18 confers broad-spectrum virus resistance in rice by sequestering a host microRNA. *eLife* **4**, e05733.
- Xie Z, Fan B, Chen C, Chen Z.** 2001. An important role of an inducible RNA-dependent RNA polymerase in plant antiviral defense. *Proceedings of the National Academy of Sciences, USA* **98**, 6516–6521.
- Yang SJ, Carter SA, Cole AB, Cheng NH, Nelson RS.** 2004. A natural variant of a host RNA-dependent RNA polymerase is associated with increased susceptibility to viruses by *Nicotiana benthamiana*. *Proceedings of the National Academy of Sciences, USA* **101**, 6297–6302.
- Yang SH, Berberich T, Sano H, Kusano T.** 2001. Specific association of transcripts of *tbzF* and *tbz17*, tobacco genes encoding basic region leucine zipper-type transcriptional activators, with guard cells of senescing leaves and/or flowers. *Plant Physiology* **127**, 23–32.
- Yin J, Chang X, Kasuga T, Bui M, Reid MS, Jiang CZ.** 2015. A basic helix-loop-helix transcription factor, PhFBH4, regulates flower senescence by modulating ethylene biosynthesis pathway in petunia. *Horticulture Research* **2**, 15059.
- Zhang X, Zhang X, Singh J, Li D, Qu F.** 2012. Temperature-dependent survival of Turnip crinkle virus-infected arabidopsis plants relies on an RNA silencing-based defense that requires *dcl2*, *AGO2*, and *HEN1*. *Journal of Virology* **86**, 6847–6854.